Original Article

Quantitative and qualitative analysis of contrast-enhanced ultrasound for differentiating benign and malignant superficial enlarged lymph nodes

Zong-Hua Yue[#], Jia-Rui Du[#], Wen-Hui Li, Han-Yu Zhang, Shao-Hua Yin, Mei-Yu Huang, Xing-Rui Liu, Guo-Qing Sui

Department of Ultrasound, China-Japan Union Hospital of Jilin University, Changchun, China

Contributions: (I) Conception and design: GQ Sui, JR Du; (II) Administrative support: GQ Sui; (III) Provision of study materials or patients: WH Li, HY Zhang; (IV) Collection and assembly of data: ZH Yue, SH Yin; (V) Data analysis and interpretation: ZH Yue, MY Huang, XR Liu; (VI) Manuscript writing: All authors; (VII) Final approval of manuscript: All authors.

[#]These authors contributed equally to this work as co-first authors.

Correspondence to: Guo-Qing Sui, MD. Department of Ultrasound, China-Japan Union Hospital of Jilin University, No. 126 Xiantai Street, Changchun 130000, China. Email: suiguoqing@jlu.edu.cn.

Background: In many clinical situations, it is critical to exclude or identify abnormally lymph nodes (LNs). The nature of superficial abnormally LNs is closely related to the stage, treatment, and prognosis of the disease. Ultrasound (US) is an important method for examining superficial LNs due to its cheap and safe characteristics. However, it is still difficult to determine the nature of some LNs with overlapping benign and malignant features in images. Contrast-enhanced ultrasound (CEUS) can be used to evaluate the microperfusion status of tissues in real time, and it can improve diagnostic accuracy to a certain extent. Therefore, in this study, we will analyze the correlation between CEUS quantitative parameters and benign and malignant superficial abnormally LNs, to evaluate the efficacy and value of CEUS in distinguishing benign and malignant superficial LNs.

Methods: This study retrospectively analyzed 120 patients of abnormal LNs who underwent US and CEUS at the China-Japan Union Hospital of Jilin University from December 2020 to August 2023. All 120 cases of abnormal LNs underwent US-guided coarse needle biopsy, and accurate pathological results were obtained, along with complete US and CEUS images. According to the pathological results, LNs were divided into benign and malignant groups, and the qualitative and quantitative parameters of US and CEUS between the two groups were analyzed. The cutoff value is determined by the receiver operating characteristic (ROC) curve of the subjects, and sensitivity, specificity, and accuracy are applied to evaluate the ability of the cutoff value to distinguish between the two groups.

Results: There were a total of 120 LNs, including 36 in the benign group and 84 in the malignant group. The results showed that malignant LNs were usually characterized by the disappearance of lymphatic hilum, round ness index (L/T) <2, irregular morphology, and the manifestation of uneven perfusion ($P<0.05$). The differences in the quantitative parameters peak enhancement (PE), rise time (RT), time to peak (TTP), wash-in rate (WIR), and wash-out rate (WOR) were statistically significant ($P<0.05$). The result showed that RT and TTP in the malignant LNs were higher than those in the benign LNs, while the PE, WIR, and WOR were lower. A comparison of the Δ values showed that the differences in ΔPE, ΔWIR, and Δfall time (FT) were statistically significant ($P<0.05$), Among them, the ΔPE and ΔWIR of malignant LNs were higher than those of benign LNs, while the ΔFT was lower than that of benign LNs.

Conclusions: Quantitative analysis of CEUS features is valuable in the diagnosis of benign and malignant LNs, and US combined with CEUS helps to improve the accuracy of identifying the nature of LNs.

© Quantitative Imaging in Medicine and Surgery. All rights reserved.

Keywords: Lymph nodes (LNs); contrast-enhanced ultrasound (CEUS); quantitative parameters

Submitted Mar 30, 2024. Accepted for publication Jul 23, 2024. Published online Aug 16, 2024.
doi: 10.21037/qims-24-658
View this article at: https://dx.doi.org/10.21037/qims-24-658

Introduction

Lymph nodes (LNs) are key immunological organs that are found throughout the body (1). In clinical practice, eliminating or recognizing LN metastases is critical in tumor staging since it directly influences patient prognosis and treatment options. It is also important to quickly identify the nature of abnormally LNs in patients without a history of cancer (2,3). The most precise way to assess questionable LNs before surgery is with a puncture biopsy. However, some LNs are too deep, close to large blood vessels, or the LNs are too small, or the patient's heart and lung functions are severely abnormal, so not all LNs being able to be biopsied (4). As a result, imaging modalities are crucial in the diagnosis of lymphadenopathy. Currently, positron emission tomography (PET), magnetic resonance imaging (MRI), computed tomography (CT), and ultrasound (US) are utilized to identify LNs. However, US is often used as the preferred method for detecting superficial LNs in clinical due to its real-time, safety and low cost (5,6).

Research has shown that for superficial LNs, contrast-enhanced ultrasound (CEUS) has greater diagnostic accuracy than US (7). As a real-time tissue perfusion assessment technique, CEUS can identify and reveal even poor tissue and lesion perfusion, providing critical information on microvascularization dynamics, which is a significant property for diagnosing and characterizing tissue abnormalities. Benign and malignant abnormalities in superficial LNs have been distinguished using CEUS in recent years (8-13). Study discovered that the increase in vascular density in LNs occurred before the alteration in LNs volume in animal models by using CEUS (14). CEUS is superior to US for revealing LNs microvessels, and it may enhance the early detection of aberrant LNs by monitoring vascular density, allowing for a more accurate categorization of LNs (15). However, as a method based on US, CEUS is limited by the experience of the operator and scanning conditions, which are the most important limitations for its widespread use as a standard diagnostic procedure (16).

The European Federation of Societies for Ultrasound in Medicine and Biology (EFSUMB) published recommendations for the quantitative analysis of CEUS in 2018 (17). Software can help quantify the blood flow perfusion characteristics of tissues, making the results of CEUS more objective and reducing dependence on operating doctor (18). Compared with other quantitative analysis software, VueBox® (Bracco, Italy) integrates different device standards to achieve multiplatform compatibility, analyzes standardized DICOM images of CEUS to obtain quantitative data, and uses color-coded maps and time-intensity curves (TICs) for detailed quantitative analysis. Perfusion parameters were obtained to examine the kinetic changes in microvasculature in lesions (19), as well as to discriminate between benign and malignant lesions (20). To assess the use of CEUS in identifying superficial LNs, we investigated the relationships between the quantitative parameters of CEUS and the benign and malignant characteristics of aberrant superficial LNs. We present this article in accordance with the STARD reporting checklist (available at https://qims.amegroups.com/article/view/10.21037/qims-24-658/rc).

Methods

The study was conducted in accordance with the Declaration of Helsinki (as revised in 2013). The study was approved by the China-Japan Union Hospital of Jilin University ethics review board (No. 2023120404) and informed consent was provided by all participants. All LNs underwent coarse needle biopsy (CNB) to obtain pathological results.

Inclusion criteria:

(I) The morphology of the LNs is abnormal under conventional US, such as enlargement, full shape, uneven internal echoes, and unclear hilum of lymph gland.
(II) CEUS was performed, and all images are saved intact as required without any omissions.
(III) Accurate pathological results can be obtained through US-guided CNB.

Exclusion criteria:

© Quantitative Imaging in Medicine and Surgery. All rights reserved.

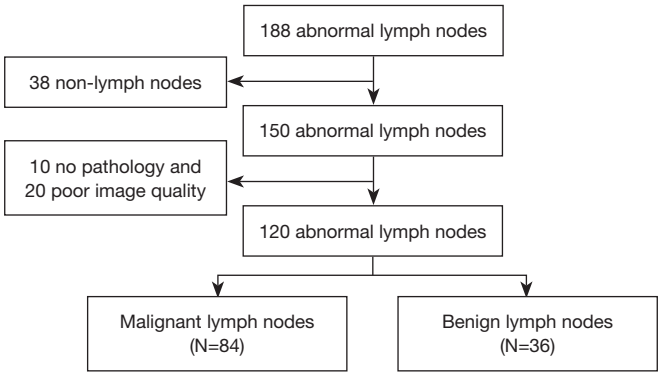

Figure 1 Flow chart of the patient selection process.

(I) The pathological results were nonlymphadenopathy.
(II) Pathological diagnosis is not accurate.
(III) Due to factors such as patient respiratory movement or probe movement, the stability of CEUS video images is poor and cannot be effectively analyzed.
(IV) CEUS was performed, but the imaging data were incomplete (missing images in some sections).
(V) Patient's allergy to contrast agent causes CEUS to be discontinued.

A total of 188 abnormal LNs from 188 consecutive patients who underwent CEUS at China-Japan Union Hospital of Jilin University from December 2020 to August 2023 were selected. Among them, the pathological results of 38 LNs are non-LNs lesions, the pathological results of 10 LNs are unclear, and the CEUS images quality of 20 LNs is poor, and ultimately 120 abnormal LNs were included in the study (*Figure 1*).

Equipment

US and CEUS were performed using Siemens (Siemens Mountainview, USA), Mindray® (Mindray, Shenzhen, China), and Supersonic (SuperSonic Imagine, France) color Doppler US diagnostic systems. All LNs were examined using the 4–9 MHZ linear array probe equipped with the machine

Conventional US and CEUS examination

The US images and CEUS videos of each LN were recorded by a doctor with more than 10 years of US experience. Images were stored digitally as Digital Imaging and Communication in Medicine (DICOM) cine loops in the axial and sagittal planes of the LNs, with a CEUS storage time of 2 minutes. The quantitative analysis of US and CEUS findings for all the LNs was performed by two doctors with more than 5 years of US diagnostic experience. The corresponding characteristics of conventional US were assessed without knowing the pathological results. These included composition (cystic, solid, mixed), echogenicity (anechoic, hyperechoic, isoechoic, hypoechoic), shape [round ness index (L/T) >2 or <2], margins (smooth or ill-defined, lobulate or irregular), and lymphatic hilum (clear or unclear), as well as quantitative ultrasonographic analysis. Two doctors independently evaluate the above variables, and in case of disagreement, the decision will be made by the higher-level doctor.

Using the sulfur hexafluoride microbubble US contrast agent (SonoVue®, Bracco, Milan, Italy), 5 mL of physiological saline was injected into the contrast agent bottle, and the contents of the bottle were shaken vigorously for 20 seconds until they were well mixed and became a milky white liquid. Three mL of configured US contrast solution was withdrawn and rapidly injected into the body via the elbow vein channel (Within 1 second), followed by rinsing with 5 mL of saline. Change to CEUS mode (mechanical index of 0.1), and the video system was turned on to record the entire imaging process.

During the imaging process, the physician is required to keep the probe stable, and the patient maintains stable breathing and dynamically observes the contrast wash-in and wash-out phases for 2 min.

Quantitative analysis of contrast US

Vuebox software was used to obtain further CEUS images (Bracco, Suisse SA, Geneva, Switzerland). The software can automatically optimize different models of US diagnostic

© Quantitative Imaging in Medicine and Surgery. All rights reserved.

systems and linear array probes, linearize DICOM, draw time intensity curves (TIC) based on region of interest (ROI), and export analysis reports. Select parameters peak enhancement (PE), wash-in area under the curve (WIAUC), rise time (RT), time to peak (TTP), wash-in rate (WIR), wash-out area under the curve (WOAUC), fall time (FT), WOR, and their corresponding Δ values (the absolute value of the difference between ROI 2 and ROI 3) for statistical analysis.

ROI is artificially selected and outlined, avoiding liquefied necrotic parts during outlined. Among them, ROI 1 is the entire region of the LN, ROI 2 is the central zone of the LN, and ROI 3 is the first enhanced part in the peripheral zone of LNs (ROI 2 and ROI 3 have equal areas), where Δ values were obtained by calculating the difference between the TIC parameters of the central and peripheral zones of the LN. The Δ value can quantitatively describe the perfusion differences between the central and peripheral regions of LNs, and objectively describe the uniformity of LN perfusion.

Starting from the first contrast agent microbubble entering the LN, analysis was conducted using dual screen mode of US and CEUS imaging. We evaluated CEUS characteristics using VueBox color-coded imaging. Dark red is the maximum PE, while dark blue is the minimum PE. The TTP and RT minimum values are shown in dark blue, while the maximum values are displayed in dark red.

Histopathological examination

All LNs underwent US-guided CNB for pathological analysis, and all LNs were categorized into benign LNs and malignant LNs based on pathological results.

Statistical analysis

The data were processed and analyzed using SPSS20.0. Qualitative variables are expressed as the number of cases and the constitutive ratio, and the chi-square test was used. We use bilateral K-S tests to verify the normality of the distribution of quantitative data. When P value is greater than the specified level of significance (5%), we consider the sample to follow a normal distribution, while conversely, the sample belongs to a skewed distribution. Measurements that satisfied the normal distribution are expressed as the mean ± standard deviation ($\overline{X}$ ± s) and analyzed using the *T*-test; measurements that did not satisfy the normal distribution are expressed as the median and interquartile spacing [M (Q1, Q3)] and analyzed using the rank-sum test for analysis; and such differences were statistically significant at P<0.05 (bilateral).

Results

Patient general characteristics

The research involved 120 patients, including 67 in the neck, 29 in the supraclavicular fossa, 9 in the axilla, and 15 in the groin, and each with a LN. For pathological investigation, an US-guided CNB was used. Based on the pathological results, the patients were categorized into benign and malignant groups, with 36 patients having benign LNs and 84 patients having malignant LNs. Among the 36 benign LNs, 10 were tuberculous LNs and 26 were inflammatory LNs, among the 84 malignant LNs, 61 were metastatic LNs (30 adenocarcinoma, 16 squamous cell carcinoma, 15 small cell carcinoma) and 23 were lymphomas (10 large B-cell lymphomas, 6 follicular lymphomas, 5 Hodgkin's lymphomas and 2 anaplastic large cell lymphomas). The participants included 60 males and 60 females with an average age of 56.9±14.17 years (range, 22–88 years).

Conventional US and CEUS results

Among 84 cases of malignant LNs, 28 showed full morphology, 41 had normal morphology, and 15 had irregular morphology. Among 36 cases of benign LNs, 9 had full morphology, and 27 had normal morphology. The difference in the three forms (full, normal, and irregular) between the two groups was significant (P=0.007; *Table 1*). Among the 84 cases of malignant LNs, 63 (75.0%) had L/T <2. Among the 36 cases of benign LNs, 20 (55.6%) had L/T <2. The difference was statistically significant (P=0.035).

In addition, 53 out of 84 cases of malignant LNs had lost lymphatic hilum and showed mixed or peripheral blood flow. Ten out of 36 cases of benign LNs had unclear lymphatic hilum and showed mixed or peripheral blood flow. The difference of lymphatic hilum status between two groups was statistically significant (P<0.001), lymphatic hilum deficiency was greater in the malignant group than in the benign group (63.1% *vs.* 27.8%).

Among 84 cases of malignant LNs, 53 showed uneven enhancement, and 31 showed uniform enhancement. Among 36 cases of benign LNs, 10 showed uneven enhancement, and 26 showed uniform enhancement. The difference was statistically significant.

© Quantitative Imaging in Medicine and Surgery. All rights reserved.

Table 1 Patient characteristics

Characteristics	No. of LNs (n=120)	Benign LNs (n=36)	Malignant LNs (n=84)	P
Gender				0.017
Male	60	12 (33.3)	48 (57.1)	
Female	60	24 (66.7)	36 (42.9)	
Lymphatic hilum				<0.001
Clear	57	26 (72.2)	31 (36.9)	
Unclear	63	10 (27.8)	53 (63.1)	
Form				0.007
Irregular	15	0 (0)	15 (17.9)	
Full	37	9 (25.0)	28 (33.3)	
Normal	68	27 (75.0)	41 (48.8)	
Long axis/short axis ratio				0.035
≥2	37	16 (44.4)	21 (25.0)	
<2	83	20 (55.6)	63 (75.0)	
Enhancement mode				0.001
Homogeneous	57	26 (72.2)	31 (36.9)	
Heterogeneous	63	10 (27.8)	53 (63.1)	

Data are presented as n or n (%). LN, lymph node.

Table 2 CEUS characteristics of benign and malignant lymph nodes

Features	Benign LNs, AUC (95% CI)	Malignant LNs, AUC (95% CI)	P
PE	14,993.00 (8,647.82–65,011.00)	8,803.53 (3,868.75–14,922.01)	<0.001
WIAUC	34,117.11 (20,019.33–85,429.57)	55,225.88 (17,791.02–124,385.35)	0.451
RT	6.34 (4.96–8.05)	8.06 (6.29–12.13)	<0.001
TTP	18.31 (14.24–21.34)	19.73 (15.97–23.63)	0.045
WIR	3,823.65 (1,079.53–8,786.38)	1,085.07 (471.64–3,429.33)	<0.001
WOAUC	64,814.44 (28,706.46–412,126.35)	93,967.18 (27,607.56–197,211.26)	0.665
FT	10.30 (7.32–16.59)	11.25 (8.53–14.73)	0.653
WOR	3,349.49 (1,189.70–6,226.85)	934.71 (310.26–2,624.05)	<0.001

CEUS, contrast-enhanced ultrasound; LN, lymph node; AUC, area under the curve; CI, confidence interval; PE, peak enhancements; WIAUC, wash-in area under the curve; RT, rise time; TTP, time to peak; WIR, wash-in rate; WOAUC, wash-out area under the curve; FT, fall time; WOR, wash-out rate.

Quantitative analysis of contrast US results

The differences in PE, RT, TTP, WIR, and WOR were statistically significant when compared between benign LNs and malignant LNs (P<0.05), RT and TTP were significantly greater in malignant LNs than in benign LNs, and PE, WIR, and WOR were significantly lower in malignant LNs than in benign LNs. In contrast, WIAUC, WOAUC, and FT were not significantly different between two groups (P>0.05) (*Table 2*). TIC showed relatively slow

© Quantitative Imaging in Medicine and Surgery. All rights reserved.

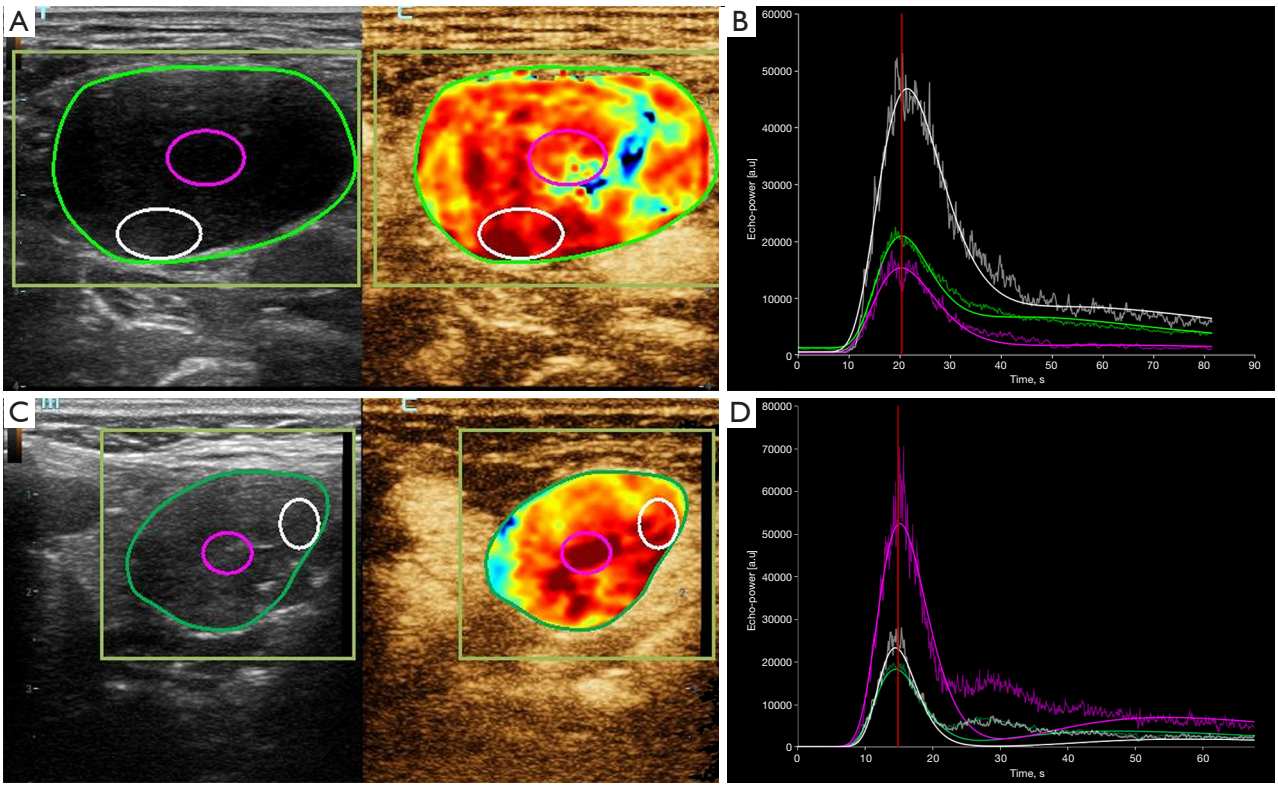

Figure 2 Vuebox analysis interface for malignant lymph nodes (A,B) and benign lymph nodes (C,D). The area enclosed by the green line is ROI 1, the area enclosed by the red line is ROI 2, and the area enclosed by the white line is ROI 3. (A,B) Male, 29 years old, a hypoechoic LN of size 3.3×2.0 cm was seen in the left supraclavicular fossa with unclear lymphatic hilum, which gradually filled with contrast agent from the periphery to the center after injection of contrast agent through the median vein of the elbow, and some areas were not filled with contrast agent microbubble. Pathological results showed that round-cell malignant tumors were seen in the perforated lymphoid tissue, and the spelling results supported germ-cell origin, which was consistent with spermatogonia. (C,D) Female, 23 years old, an elliptical LN of about 3.17×1.62 cm in size was seen in the left cervical region II, the lymphatic hilum was still clear, and the lesion showed homogeneous hyper-enhancement after injection of contrast agent through the median vein of the elbow. Pathological results showed that the lymphatic sinus was dilated in the punctured lymphoid tissue, and lobulated nucleated cells and plasma cells were seen in and around the sinus, which was considered reactive hyperplasia. a.u. signal intensity parameters in arbitrary units; ROI, region of interest; LN, lymph node.

and low enhancement of malignant LNs in the arterial phase compared to benign LNs (*Figure 2*).

A comparison of the Δ values of the TIC parameters between benign and malignant LNs revealed that the differences in ΔPE, ΔWIR, and ΔFT were statistically significant (P<0.05). Specifically, the ΔPE and ΔWIR of malignant LNs were significantly greater than those of benign LNs, the ΔFT of malignant LNs was significantly lower than that of benign LNs, and the remaining parameters were not significantly different between the two groups (P>0.05) (*Table 3*). TIC analysis of the Δ values showed that malignant LNs had relatively greater enhancement in the arterial phase than benign LNs did.

Diagnostic efficacy of the quantitative parameters

All 120 abnormal LNs were analyzed using Vuebox, and the receiver operating characteristic (ROC) curves (*Figure 3A*) showed that the area under the curve (AUC) for PE was 0.724 (0.630–0.818, P<0.001), and the best threshold value for predicting malignant LNs was 7,391.125 signal intensity parameters in arbitrary units (a.u.) (sensitivity of 44.0%, specificity of 94.4%). The AUC for RT was 0.722 (0.627–0.817, P<0.001), and the best cutoff value for predicting malignant LNs was 9.1 s (sensitivity 42.9%, specificity 91.7%). The diagnostic efficacy for malignant LNs was better when the cutoff value of PE combined with lymphatic

© Quantitative Imaging in Medicine and Surgery. All rights reserved.

Table 3 Comparison of TIC parameters Δ values in benign and malignant lymph nodes

Features	Benign LNs, AUC (95% CI)	Malignant LNs, AUC (95% CI)	P
ΔPE	5,109.67 (1,570.40–21,011.79)	10,181.03 (3,870.49–42,438.61)	0.047
ΔWIAUC	24,879.16 (10,960.51–90,116.15)	38,272.09 (17,986.84–133,697.89)	0.134
ΔRT	1.23 (0.35–2.10)	0.98 (0.28–2.34)	0.622
ΔTTP	0.92 (0.44–1.54)	0.92 (0.34–2.32)	0.656
ΔWIR	893.88 (236.28–3,246.79)	2,435.95 (729.33–6,586.33)	0.032
ΔWOAUC	33,408.32 (16,218.30–107,964.12)	50,666.39 (24,055.58–191,958.87)	0.077
ΔFT	3.80 (2.47–6.60)	1.96 (0.59–3.39)	<0.001
ΔWOR	566.63 (230.40–2,149.76)	1,328.06 (313.99–4,202.95)	0.217

TIC, time-intensity curve; Δ values, absolute value of the difference between ROI 2 and ROI 3; LN, lymph node; AUC, area under the curve; CI, confidence interval; PE, peak enhancements; WIAUC, wash-in area under the curve; RT, rise time; TTP, time to peak; WIR, wash-in rate; WOAUC, wash-out area under the curve; FT, fall time; WOR, wash-out rate; ROI, region of interest.

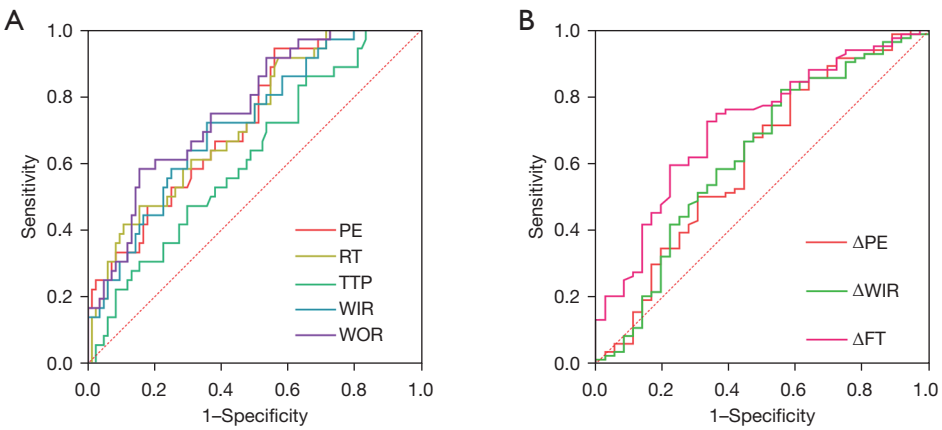

Figure 3 ROC curve for evaluating the diagnostic efficacy of TIC parameters in benign and malignant lymph nodes by CEUS. (A) The ROC curve of the CEUS value. (B) The ROC curve of the Δ value. PE, peak enhancement; RT, rise time; TTP, time to peak; WIR, wash-in rate; WOR, wash-out rate; FT, fall time; ROC, receiver operating characteristic; TIC, time-intensity curve; CEUS, contrast-enhanced ultrasound.

hilum was 7,167.97 a.u. The sensitivity, specificity, and AUC for quantitative analysis of PE combined with lymphatic hilum by CEUS were 79.8%, 77.8%, and 0.813, respectively (*Table 4*).

According to the ROCs of the Δ value, it has a better diagnostic effect on LNs when the cutoff value of Δ PE was 3,278.295 a.u. (0.499–0.730, P=0.047) (*Figure 3B*). Quantitative CEUS analysis revealed that ΔPE had a sensitivity of 82.1%, a specificity of 41.7%, and an AUC of 0.615. The diagnosis of LNs was better when the ΔWIR cutoff value was 575.185 a.u. (0.508–0.739, P=0.032), and quantitative CEUS analysis revealed that the sensitivity of the ΔWIR was 82.1%, the specificity was 44.4%, and the AUC was 0.624. The diagnosis of LNs was better when the cutoff value of ΔFT was 3.22 s (0.614–0.813, P<0.001), and quantitative analysis by CEUS showed that ΔFT had a sensitivity of 72.6%, a specificity of 66.7%, and an AUC of 0.713 (*Table 5*).

Discussion

Diagnosing benign or malignant LNs is critical for clinical diagnosis and therapy. The state of the LNs is an essential indicator for assessing the prognosis of

© Quantitative Imaging in Medicine and Surgery. All rights reserved.

Table 4 ROC curve table

Features	Sensitivity (%)	Specificity (%)	Accuracy (%)	AUC (95% CI)	P
PE	44.0	94.4	72.4	0.724 (0.630–0.818)	<0.001
RT	42.9	91.7	72.2	0.722 (0.627–0.817)	<0.001
TTP	34.5	86.1	61.6	0.616 (0.510–0.722)	0.045
WIR	64.3	72.2	71.8	0.718 (0.621–0.814)	<0.001
WOR	84.5	58.3	76.2	0.762 (0.673–0.850)	<0.001

The area under the ROC curve was greater than 0.05, suggesting that the diagnostic test had certain diagnostic significance. ROC, receiver operating characteristic; AUC, area under the curve; CI, confidence interval; PE, peak enhancements; RT, rise time; TTP, time to peak; WIR, wash-in rate; WOR, wash-out rate.

Table 5 ROC curve table of Δ value

Features	Sensitivity (%)	Specificity (%)	Accuracy (%)	AUC (95% CI)	P
ΔPE	82.1	41.7	61.5	0.615 (0.499–0.730)	0.047
ΔWIR	82.1	44.4	62.4	0.624 (0.508–0.739)	0.032
ΔFT	72.6	66.7	71.3	0.713 (0.614–0.813)	<0.001

The area under the ROC curve was greater than 0.05, suggesting that the diagnostic test had certain diagnostic significance. ROC, receiver operating characteristic; Δ values, absolute value of the difference between ROI 2 and ROI 3; AUC, area under the curve; CI, confidence interval; PE, peak enhancements; WIR, wash-in rate; FT, fall time; ROI, region of interest.

patients with malignancies. Puncture biopsy is the most reliable procedure for the preoperative examination of questionable LNs; nonetheless, it is an intrusive test that is not recommended for every aberrant LN. Thus, reducing the number of patients needing biopsy would be the ideal outcome for increasing the diagnostic accuracy of LN analysis.

The size of the LNs alone cannot reliably indicate benign or malignant LNs since they are often impacted by many factors (21). Furthermore, the appearance of LNs and the existence or lack of lymphatic hilum might serve as indicators of whether a node is benign or cancerous (22,23). However, the diagnostic features of conventional US are not absolute and have certain limitations. Currently, CEUS is useful in the differential diagnosis of aberrant LNs since it is a real-time method for evaluating tissue perfusion (24,25). The sensitivity and specificity of neovascularization in malignant LNs are greatly enhanced by CEUS (26). It has been reported that its resolution may exceed that of CT and MRI (27), suggesting that US is valuable for detecting abnormal LNs (28). Our study showed that most malignant LNs (63.1%) showed uneven enhancement on US, whereas most benign LNs (72.2%) showed uniform enhancement. Previous studies have shown uniform enhancement in benign LNs and uneven enhancement and perfusion defects in most malignant LNs (29,30), which is consistent with the results of the present study and suggests that there is some similarity in the angiographic perfusion characteristics of malignant LNs. This might be because immature neovascularization and avascular necrotic regions are frequent in malignant LNs and obstruct the distribution of the contrast agent, resulting in perfusion deficiencies. On the other hand, in the majority of benign LNs, contrast microbubbles demonstrate uniform enhancement and quickly flow from the lymphatic hilum to the surrounding area of LN (31-33). However, 36.9% of malignant LNs showed uniform enhancement, and 27.8% of benign LNs showed uneven enhancement. This implies that the qualitative diagnosis of LNs by CEUS has limitations. Although necrosis is often considered a sign of malignancy, necrosis alone does not indicate malignant LNs. Tuberculosis, inflammation, and other lesions may also result in necrosis. These unusual sonographic symptoms may limit the specificity of CEUS for determining whether aberrant LNs are benign or malignant.

To measure changes in microvascularization kinetics, objective parameters of US are thus needed. Scheipers *et al.* demonstrated that a computer-guided self-learning analytic

© Quantitative Imaging in Medicine and Surgery. All rights reserved.

system might be useful for locating categorization traits that are independent of the investigator (34). The TIC curves obtained by processing and analyzing the data using quantitative analysis software such as Vuebox can provide an objective diagnostic basis. Nie *et al.* (35) performed a quantitative analysis of PE and RT and combined the results with the results of US images in contrast perfusion and enhancement modes to improve the accuracy of the differential diagnosis of head and neck LNs. Ying *et al.* (22) used time-of-arrival parametric imaging to examine the arrival time (AT) of the contrast agent around LNs to provide additional information for the differential diagnosis of superficial LNs (36). The AUC, FT, PE, and RT are now the primary clinical quantitative analytic metrics for ultrasonographic TIC parameters. PE and AUC quantitative analysis may indicate the contrast concentration of contrast agent perfusion, and RT and FT can reflect the efficiency of contrast agent washout, which can provide significant diagnostic information for various kinds of lesions (37). Although PE, RT, and FT are significant TIC metrics, we think that the information obtained by analyzing only 3 parameters may not be complete. Therefore, we analyzed more parameters of LNs blood perfusion in this study.

This study retrospectively analyzed CEUS images of 120 LNs with abnormal routine US findings to construct TICs. Quantitative parameters were extracted from the TICs of several ROI, including PE, TTP, WIAUC, RT, WIR, WOAUC, FT, WOR, among which WIAUC, RT, WIR objectively reflect the wash-in of contrast agent, WOAUC, FT, WOR objectively reflect the wash-out of contrast agent, TTP is the time of peak concentration of contrast agent, and PE is the peak intensity (PI) of contrast agent.

In our study, RT and TTP were significantly greater in malignant LNs than in benign LNs; PE, WIR, and WOR were significantly lower in malignant LNs than in benign LNs. The ROC curve revealed a diagnostic effectiveness of 0.724 for peak-intensity PE, with a sensitivity of 44.0% and a specificity of 94.4%. The diagnostic efficacy of RT in the wash-in phase was the highest at 0.722, with a sensitivity of 42.9% and a specificity of 91.7%. The highest diagnostic efficacy of the WOR in the washout phase was 0.762, with a sensitivity of 84.5% and a specificity of 58.3%. The features of "low enhancement, slow wash-in, and delayed wash-out" in malignant LNs may be associated with LN malignancy. Reduced wash-in, decreased PE, and inadequate blood supply are the outcomes of malignant LN core blood vessel compression due to the lack of normal structure. Moreover, mesangial growth factors in malignant LNs give rise to large number of twisted immature microvessels that are irregular in caliber and have incomplete vessel walls. Because of the irregular morphology of these vessels, blood flow is irregular, and stasis and turbulence may occur (38,39), thus increasing the distance of contrast in and out of the tumor. Tumor infiltration may result in neovascularization stenosis or occlusion along with temporal stromal edema fibrosis. In addition, it has been suggested that the slow decline in the TIC in malignant LNs may be related to disturbed tumor venous feedback (40). Previous research has quantified the benign and malignant nature of aberrant LNs; however, the findings of these investigations are inconsistent. Jiang *et al.* (41) showed that the PI of malignant LNs was significantly greater than that of normal LNs, while Chen *et al.* (31) quantitatively analyzed 55 cases of abnormal LNs and found no statistically significant differences in quantitative parameters such as the PI, TTP, MTT, or RT between the two groups; these differences are likely due to the small sample size and differences in the analysis methods used. lymphatic hilum absence is one of the most common signs of malignancy according to US (23), and ROC-based assessment combined with quantitative CEUS analysis of the PI and lymphatic hilum provided good diagnostic results for the identification of abnormal LNs (sensitivity, specificity, and AUC of 79.8%, 77.8%, and 0.813, respectively); however, the addition of LNs morphologic features slightly improved the diagnostic performance (0.724 *vs.* 0.813), and the specificity was lower (94.4% *vs.* 77.8%).

Furthermore, the Δ value may provide more objective diagnostic information and help prevent diagnostic mistakes caused by individual variances across patients (42). Our research examined the efficacy of the TIC parameter Δvalue, or the difference between the TIC parameter in the central and peripheral zones of the LNs, as a diagnostic tool for differentiating between benign and malignant LNs. The results showed that the ΔPE and ΔWIR of malignant LNs were significantly greater than those of benign LNs, and the ΔFT of malignant LNs was significantly lower than that of benign LNs. The ROC curve showed a diagnostic efficacy of 0.615 for PI ΔPE, with a sensitivity of 82.1% and a specificity of 41.7%. The diagnostic efficacy of the ΔWIR in the wash-in phase was 0.624, with a sensitivity of 82.1% and a specificity of 44.4%. The diagnostic efficacy of ΔFT in the washout phase was 0.713, with a sensitivity of 72.6% and a specificity of 66.7%. Malignant LNs were further confirmed to have lower enhancement and slower wash-in and wash-out times than benign LNs. Our results are consistent with those of Nemec *et al.* and Hu *et al.* (43,44).

© Quantitative Imaging in Medicine and Surgery. All rights reserved.

This study has several limitations. This was a retrospective study, for instance. Furthermore, this was a single-center study with a small sample size; larger multicenter patient recruitment will be a feature of future research.

Conclusions

Quantitative examination of CEUS characteristics is useful for qualitatively diagnosing abnormal LNs, and our findings demonstrate that malignant LNs on CEUS display modest enhancement, sluggish wash-in, and delayed wash-out. RT and TTP were significantly greater in malignant LNs than in benign LNs; PE, WIR, and WOR were significantly lower in malignant LNs than in benign LNs. Furthermore, the Δ value may provide more objective diagnostic information. ΔPE and ΔWIR of malignant LNs were significantly greater than those of benign LNs, and the ΔFT of malignant LNs was significantly lower than that of benign LNs. Additional studies with larger sample sizes should be performed in the future to confirm our findings and determine whether imaging histology models that include CEUS characteristics could help doctors distinguish between benign and malignant LNs.

Acknowledgments

The authors thank the volunteers who participated in this study.
Funding: This work was supported by the Department of Finance of Jilin Province (grant No. 3D5206055430).

Footnote

Reporting Checklist: The authors have completed the STARD reporting checklist. Available at https://qims.amegroups.com/article/view/10.21037/qims-24-658/rc

Conflicts of Interest: All authors have completed the ICMJE uniform disclosure form (available at https://qims.amegroups.com/article/view/10.21037/qims-24-658/coif). The authors have no conflicts of interest to declare.

Ethical Statement: The authors are accountable for all aspects of the work in ensuring that questions related to the accuracy or integrity of any part of the work are appropriately investigated and resolved. The study was conducted in accordance with the Declaration of Helsinki (as revised in 2013). The study was approved by the China-Japan Union Hospital of Jilin University ethics review board (No. 2023120404) and informed consent was provided by all participants.

Open Access Statement: This is an Open Access article distributed in accordance with the Creative Commons Attribution-NonCommercial-NoDerivs 4.0 International License (CC BY-NC-ND 4.0), which permits the non-commercial replication and distribution of the article with the strict proviso that no changes or edits are made and the original work is properly cited (including links to both the formal publication through the relevant DOI and the license). See: https://creativecommons.org/licenses/by-nc-nd/4.0/.

References

1. Gasteiger G, Ataide M, Kastenmüller W. Lymph node - an organ for T-cell activation and pathogen defense. Immunol Rev 2016;271:200-20.
2. Slaisova R, Benda K, Jarkovsky J, Petrasova H, Szturz P, Valek V. Contrast-enhanced ultrasonography compared to gray-scale and power doppler in the diagnosis of peripheral lymphadenopathy. Eur J Radiol 2013;82:693-8.
3. Struckmeier AK, Buchbender M, Lutz R, Agaimy A, Kesting M. Comparison of the prognostic value of lymph node yield, lymph node ratio, and number of lymph node metastases in patients with oral squamous cell carcinoma. Head Neck 2024;46:1083-93.
4. Chmiel P, Krotewicz M, Szumera-Ciećkiewicz A, Bartnik E, Czarnecka AM, Rutkowski P. Review on Lymph Node Metastases, Sentinel Lymph Node Biopsy, and Lymphadenectomy in Sarcoma. Curr Oncol 2024;31:307-23.
5. Ying M, Ahuja A. Sonography of neck lymph nodes. Part I: normal lymph nodes. Clin Radiol 2003;58:351-8.
6. Ling W, Nie J, Zhang D, Yang Q, Jin H, Ou X, Ma X, Luo Y. Role of Contrast-Enhanced Ultrasound (CEUS) in the Diagnosis of Cervical Lymph Node Metastasis in Nasopharyngeal Carcinoma (NPC) Patients. Front Oncol 2020;10:972.
7. Yu M, Liu Q, Song HP, Han ZH, Su HL, He GB, Zhou XD. Clinical application of contrast-enhanced ultrasonography in diagnosis of superficial lymphadenopathy. J Ultrasound Med 2010;29:735-40.
8. Fang F, Gong Y, Liao L, Ye F, Zuo Z, Li X, Zhang Q, Tang K, Xu Y, Zhang R, Chen S, Niu C. Value of Contrast-Enhanced Ultrasound for Evaluation of Cervical Lymph Node Metastasis in Papillary Thyroid Carcinoma. Front Endocrinol (Lausanne) 2022;13:812475.

© Quantitative Imaging in Medicine and Surgery. All rights reserved.

9. Wang T, Xu M, Xu C, Wu Y, Dong X. Comparison of microvascular flow imaging and contrast-enhanced ultrasound for blood flow analysis of cervical lymph node lesions. Clin Hemorheol Microcirc 2023;85:249-59.
10. Poanta L, Serban O, Pascu I, Pop S, Cosgarea M, Fodor D. The place of CEUS in distinguishing benign from malignant cervical lymph nodes: a prospective study. Med Ultrason 2014;16:7-14.
11. Rubaltelli L, Beltrame V, Scagliori E, Bezzon E, Frigo AC, Rastrelli M, Stramare R. Potential use of contrast-enhanced ultrasound (CEUS) in the detection of metastatic superficial lymph nodes in melanoma patients. Ultraschall Med 2014;35:67-71.
12. Spiesecke P, Neumann K, Wakonig K, Lerchbaumer MH. Contrast-enhanced ultrasound (CEUS) in characterization of inconclusive cervical lymph nodes: a meta-analysis and systematic review. Sci Rep 2022;12:7804.
13. Mei M, Ye L, Quan J, Huang P. Contrast-enhanced ultrasound for the differential diagnosis between benign and metastatic superficial lymph nodes: a meta-analysis. Cancer Manag Res 2018;10:4987-97.
14. Sato T, Takemura T, Ouchi T, Mori S, Sakamoto M, Arai Y, Kodama T. Monitoring of Blood Vessel Density Using Contrast-Enhanced High Frequency Ultrasound May Facilitate Early Diagnosis of Lymph Node Metastasis. J Cancer 2017;8:704-15.
15. Liu J, Liu X, He J, Gou B, Luo Y, Deng S, Wen H, Zhou L. Percutaneous contrast-enhanced ultrasound for localization and diagnosis of sentinel lymph node in early breast cancer. Sci Rep 2019;9:13545.
16. Putz FJ, Verloh N, Erlmeier A, Schelker RC, Schreyer AG, Hautmann MG, Stroszczynski C, Banas B, Jung EM. Influence of limited examination conditions on contrast-enhanced sonography for characterising liver lesions. Clin Hemorheol Microcirc 2019;71:267-76.
17. Sidhu PS, Cantisani V, Dietrich CF, Gilja OH, Saftoiu A, Bartels E, et al. The EFSUMB Guidelines and Recommendations for the Clinical Practice of Contrast-Enhanced Ultrasound (CEUS) in Non-Hepatic Applications: Update 2017 (Long Version). Ultraschall Med 2018;39:e2-e44.
18. Radzina M, Ratniece M, Putrins DS, Saule L, Cantisani V. Performance of Contrast-Enhanced Ultrasound in Thyroid Nodules: Review of Current State and Future Perspectives. Cancers (Basel) 2021;13:5469.
19. Tranquart F, Mercier L, Frinking P, Gaud E, Arditi M. Perfusion quantification in contrast-enhanced ultrasound (CEUS)--ready for research projects and routine clinical use. Ultraschall Med 2012;33 Suppl 1:S31-8.
20. Wiesinger I, Jung F, Jung EM. Contrast-enhanced ultrasound (CEUS) and perfusion imaging using VueBox®. Clin Hemorheol Microcirc 2021;78:29-40.
21. Giacomini CP, Jeffrey RB, Shin LK. Ultrasonographic evaluation of malignant and normal cervical lymph nodes. Semin Ultrasound CT MR 2013;34:236-47.
22. Ying M, Bhatia KS, Lee YP, Yuen HY, Ahuja AT. Review of ultrasonography of malignant neck nodes: greyscale, Doppler, contrast enhancement and elastography. Cancer Imaging 2014;13:658-69.
23. Bialek EJ, Jakubowski W, Szczepanik AB, Maryniak RK, Prochorec-Sobieszek M, Bilski R, Szopinski KT. Vascular patterns in superficial lymphomatous lymph nodes: A detailed sonographic analysis(). J Ultrasound 2007;10:128-34.
24. Rubaltelli L, Khadivi Y, Tregnaghi A, Stramare R, Ferro F, Borsato S, Fiocco U, Adami F, Rossi CR. Evaluation of lymph node perfusion using continuous mode harmonic ultrasonography with a second-generation contrast agent. J Ultrasound Med 2004;23:829-36.
25. Rubaltelli L, Beltrame V, Tregnaghi A, Scagliori E, Frigo AC, Stramare R. Contrast-enhanced ultrasound for characterizing lymph nodes with focal cortical thickening in patients with cutaneous melanoma. AJR Am J Roentgenol 2011;196:W8-12.
26. Wang Y, Wang W, Li J, Tang J. Gray-scale contrast-enhanced ultrasonography of sentinel lymph nodes in a metastatic breast cancer model. Acad Radiol 2009;16:957-62.
27. Dudau C, Hameed S, Gibson D, Muthu S, Sandison A, Eckersley RJ, Clarke P, Cosgrove DO, Lim AK. Can contrast-enhanced ultrasound distinguish malignant from reactive lymph nodes in patients with head and neck cancers? Ultrasound Med Biol 2014;40:747-54.
28. Weskott HP. Contrast-enhanced ultrasound in the diagnostic workup of lymph nodes. Radiologe 2018;58:563-71.
29. Xiang D, Hong Y, Zhang B, Huang P, Li G, Wang P, Li Z. Contrast-enhanced ultrasound (CEUS) facilitated US in detecting lateral neck lymph node metastasis of thyroid cancer patients: diagnosis value and enhancement patterns of malignant lymph nodes. Eur Radiol 2014;24:2513-9.
30. Zhao J, Zhang J, Zhu QL, Jiang YX, Sun Q, Zhou YD, Wang MQ, Meng ZL, Mao XX. The value of contrast-enhanced ultrasound for sentinel lymph node identification and characterisation in pre-operative breast cancer patients: A prospective study. Eur Radiol 2018;28:1654-61.

© Quantitative Imaging in Medicine and Surgery. All rights reserved.

31. Chen L, Chen L, Liu J, Wang B, Zhang H. Value of Qualitative and Quantitative Contrast-Enhanced Ultrasound Analysis in Preoperative Diagnosis of Cervical Lymph Node Metastasis From Papillary Thyroid Carcinoma. J Ultrasound Med 2020;39:73-81.
32. Hong YR, Luo ZY, Mo GQ, Wang P, Ye Q, Huang PT. Role of Contrast-Enhanced Ultrasound in the Preoperative Diagnosis of Cervical Lymph Node Metastasis in Patients with Papillary Thyroid Carcinoma. Ultrasound Med Biol 2017;43:2567-75.
33. Wei Y, Yu MA, Niu Y, Hao Y, Di JX, Zhao ZL, Cao XJ, Peng LL, Li Y. Combination of Lymphatic and Intravenous Contrast-Enhanced Ultrasound for Evaluation of Cervical Lymph Node Metastasis from Papillary Thyroid Carcinoma: A Preliminary Study. Ultrasound Med Biol 2021;47:252-60.
34. Scheipers U, Siebers S, Gottwald F, Ashfaq M, Bozzato A, Zenk J, Iro H, Ermert H. Sonohistology for the computerized differentiation of parotid gland tumors. Ultrasound Med Biol 2005;31:1287-96.
35. Nie J, Ling W, Yang Q, Jin H, Ou X, Ma X. The Value of CEUS in Distinguishing Cancerous Lymph Nodes From the Primary Lymphoma of the Head and Neck. Front Oncol 2020;10:473.
36. Yin SS, Cui QL, Fan ZH, Yang W, Yan K. Diagnostic Value of Arrival Time Parametric Imaging Using Contrast-Enhanced Ultrasonography in Superficial Enlarged Lymph Nodes. J Ultrasound Med 2019;38:1287-98.
37. Xin L, Yan Z, Zhang X, Zang Y, Ding Z, Xue H, Zhao C. Parameters for Contrast-Enhanced Ultrasound (CEUS) of Enlarged Superficial Lymph Nodes for the Evaluation of Therapeutic Response in Lymphoma: A Preliminary Study. Med Sci Monit 2017;23:5430-8.
38. Schroeder RJ, Bostanjoglo M, Rademaker J, Maeurer J, Felix R. Role of power Doppler techniques and ultrasound contrast enhancement in the differential diagnosis of focal breast lesions. Eur Radiol 2003;13:68-79.
39. Nakopoulou L, Stefanaki K, Panayotopoulou E, Giannopoulou I, Athanassiadou P, Gakiopoulou-Givalou H, Louvrou A. Expression of the vascular endothelial growth factor receptor-2/Flk-1 in breast carcinomas: correlation with proliferation. Hum Pathol 2002;33:863-70.
40. Cui XW, Jenssen C, Saftoiu A, Ignee A, Dietrich CF. New ultrasound techniques for lymph node evaluation. World J Gastroenterol 2013;19:4850-60.
41. Jiang W, Wei HY, Zhang HY, Zhuo QL. Value of contrast-enhanced ultrasound combined with elastography in evaluating cervical lymph node metastasis in papillary thyroid carcinoma. World J Clin Cases 2019;7:49-57.
42. Liu Y, Chen J, Zhang C, Li Q, Zhou H, Zeng Y, Zhang Y, Li J, Xv W, Li W, Zhu J, Zhao Y, Chen Q, Huang Y, Li H, Huang Y, Yang G, Huang P. Ultrasound-Based Radiomics Can Classify the Etiology of Cervical Lymphadenopathy: A Multi-Center Retrospective Study. Front Oncol 2022;12:856605.
43. Nemec U, Nemec SF, Novotny C, Weber M, Czerny C, Krestan CR. Quantitative evaluation of contrast-enhanced ultrasound after intravenous administration of a microbubble contrast agent for differentiation of benign and malignant thyroid nodules: assessment of diagnostic accuracy. Eur Radiol 2012;22:1357-65.
44. Hu Y, Li P, Jiang S, Li F. Quantitative analysis of suspicious thyroid nodules by contrast-enhanced ultrasonography. Int J Clin Exp Med 2015;8:11786-93.

Cite this article as: Yue ZH, Du JR, Li WH, Zhang HY, Yin SH, Huang MY, Liu XR, Sui GQ. Quantitative and qualitative analysis of contrast-enhanced ultrasound for differentiating benign and malignant superficial enlarged lymph nodes. Quant Imaging Med Surg 2024;14(9):6362-6373. doi: 10.21037/qims-24-658

© Quantitative Imaging in Medicine and Surgery. All rights reserved.